Original Article
OBESITY BIOLOGY AND INTEGRATED PHYSIOLOGY

Obesity

Obesity Depresses the Anti-Inflammatory HSP70 Pathway, Contributing to NAFLD Progression

Fábio Cangeri Di Naso[1], Rossana Rosa Porto[2,3], Henrique Sarubbi Fillmann[1,4], Lucas Maggioni[4], Alexandre Vontobel Padoin[4], Rafael Jacques Ramos[4], Claudio Corá Mottin[4], Aline Bittencourt[2,3], Norma Anair Possa Marroni[1,5], and Paulo Ivo Homem de Bittencourt Jr[2,3]*

Objectives: To evaluate whether reduced activity of the anti-inflammatory HSP70 pathway correlates with nonalcoholic fatty liver disease (NAFLD) progression and with markers of oxidative stress because obesity activates inflammatory JNKs, whereas HSP70 exerts the opposite effect.

Methods: Adult obese patients ($N = 95$) undergoing bariatric surgery were divided into steatosis (ST), steatohepatitis (SH), and fibrosis (SH+F) groups. The levels of HSP70, its major transcription factor, HSF1, and JNKs were assessed by immunoblotting hepatic and visceral adipose tissue; data were confirmed by immunohistochemistry. Plasma biochemistry (lipids, HbA_{1c}, HOMA, hepatic enzymes, and redox markers) was also evaluated.

Results: In both liver and adipose tissue, decreased HSP70 levels, paralleled by similar reductions in HSF1 and reduced plasma antioxidant enzyme activities, correlated with insulin resistance and with NAFLD progression (expression levels were as follows: $ST > SH > SH + F$). The immunohistochemistry results suggested Kupffer cells as a site of HSP70 inhibition. Conversely, JNK1 content and phosphorylation increased.

Conclusions: Decreased HSF1 levels in the liver and fat of obese patients correlated with impairment of HSP70 in an NAFLD stage-dependent manner. This impairment may affect HSP70-dependent anti-inflammation, with consequent oxidative stress and insulin resistance in advanced stages of NAFLD. Possible causal effects of fat cell senescence are discussed.

Obesity (2015) **23**, 120-129. doi:10.1002/oby.20919

Introduction

The increasing worldwide prevalence of obesity and high fasting glucose concentrations, which are interdependent risk factors for nonalcoholic fatty liver disease (NAFLD), have become a major healthcare problem (1). Additionally, NAFLD encompasses a broad spectrum of successive and progressive pathological conditions that circumscribe hepatic steatosis, its inflammatory variant, nonalcoholic steatohepatitis (NASH), progressive fibrosis, cirrhosis and, eventually, hepatocellular carcinoma (2).

Because obesity is accompanied by an inflammatory status in metabolic tissues (3) and because adipose tissue-derived hormones influence hepatic function, as observed in mouse models of NAFLD (4), the crosstalk between fat and the liver has been the subject of much attention (5,6). Visceral adipose tissue is inherently pro-inflammatory, although inflammation has also been observed in stressed subcutaneous adipose tissue in a rat model of obesity (7). Important consequences include the release of macrophage cytokines, namely, macrophage chemotactic protein 1 (MCP-1) and tumor necrosis factor-α (TNFα) (8). Moreover,

[1] Laboratory of Physiology and Experimental Hepatology, Porto Alegre Clinics Hospital, Federal University of Rio Grande do Sul (UFRGS), Porto Alegre, Brazil [2] Laboratory of Cellular Physiology, Institute of Basic Health Sciences, Federal University of Rio Grande do Sul, Porto Alegre, RS, Brazil [3] National Institute of Hormones and Women's Health, Porto Alegre, Brazil [4] Center of Obesity and Metabolic Surgery, São Lucas Hospital, Pontifical Catholic University of Rio Grande do Sul (PUCRS), Brazil [5] Lutheran University of Brazil, ULBRA, Brazil. Correspondence: Norma A. P. Marroni (nmarroni@terra.com.br) and Paulo I. Homem de Bittencourt (pauloivo@ufrgs.br).

Funding agencies: PIHBJ and NPM received grant support from the Brazilian National Council for Scientific and Technological Development (CNPq, grant "Heat Shock Protein Metabolism in Diabetes" #563870/2010-9, 402626/2012-5 and 402364/2012-0 to PIHBJ) and from the Porto Alegre Clinics Hospital (FIPE HCPA #08-534 and ULBRA to NPM), which funded the present work.

Disclosure: The authors declare no conflict of interest and no competing financial interests in relation to the described work.

Author Contribution: FCN, RRP, and AB completed all the experiments described in this manuscript. HSF, CCM, AVP, and RJR performed the surgeries. All authors were involved in analyzing the results. FCN, PIHBJ, and NPM co-wrote the article. FCN, PIHBJ, and NPM designed the study. PIHBJ and NPM provided experimental advice and helped with revising the manuscript. All the authors had final approval of the submitted and published versions.

*Fábio Cangeri Di Naso and Rossana Rosa Porto contributed equally to this work.

Additional Supporting Information may be found in the online version of this article.

Received: 6 March 2014; **Accepted:** 12 September 2014; **Published online 8 October 2014. doi:10.1002/oby.20919**

TABLE 1 Anthropometric features and plasma parameters of all enrolled fasting nonalcoholic fatty liver disease (NAFLD) obese patients

	Groups			ANOVA *P* values and comparisons			
Variables	ST	SH	SH+F	*ANOVA*	*STxSH*	*STxSH+F*	*SHxSH+F*
N **(%)**	27(28.4%)	38(40%)	30(31.6%)				
Age (years)	33.78 ± 7.99	38.71 ± 10.02	39.00 ± 9.97	0.081	ns	ns	ns
Sex (female/male)	26/1	29/9	20/10	-	-	-	-
SAH prevalence (%)	7.4%	60.5%	56.0%	0.001	0.001	0.001	ns
BMI (kg m^{-2})	44.56 ± 7.83	46.71 ± 8.38	47.54 ± 6.75	0.331	ns	ns	ns
Waist circumference (cm)	135.82 ± 12,63	137.83 ± 14.49	137,11 ± 14,28	0.149	ns	ns	ns
Body fat (%)	51.66 ± 2.16	49.03 ± 6.43	48.39 ± 11.23	0.647	ns	ns	ns
Obesity degree (%)	196.87 ± 20.13	199.92 ± 22.51	205.27 ± 27.02	0.796	ns	ns	ns
AST (U l^{-1})	23.37±10.29	27.92±10.12	35.10±19.36	0.007	ns	0.005	ns
ALT (U i^{-1})	24.55±10.13	38.89±18.41	51.40±46.55	0.003*	0.005	0.01	ns
Albumin (g dl^{-1})	4.15±0.32	4.13± 0.35	4.28±1.10	ns			
Platelets/mm^3	278.29±44.08	273.34±55.06	273.16±44.53	ns			
NAFLD fibrosis score	2.45± 0.76	2.99 ± 1.03	4.87 ± 0.88	0.001	ns	0.001	0.002
Cholesterol (mM)	5.04 ± 0.79	5.19 ± 1.01	4.93 ± 1.17	0.575	ns	ns	ns
HDL-c (mM)	1.25 ± 0.25	1.25 ± 0.28	1.28 ± 0.28	0.865	ns	ns	ns
LDL-c (mM)	3.05 ± 0.82	3.17 ± 0.87	2.85 ± 0.87	0.395	ns	ns	ns
TAG (mM)	1.76 ± 1.38	1.99 ± 1.23	1.85 ± 0.77	0.732	ns	ns	ns
Diabetes (%)	9(33.3%)	29 (74.4%)	23(79.3%)	0.05	0.05	0.05	ns
Metformin treatment (%)	14.3%	34.21%	30.0%	-	-	-	-
Insulin treatment (%)	14.3%	7.9%	1.0%	-	-	-	-
Glycemia (mM)	5.18 ± 1.03	6.69 ± 2.80	5.97 ± 1.26	0.019*	0.015	0.04	ns
Insulinemia (pM)	152.6 ±85.4	224.7 ± 115.9	229.4 ± 87.1	0.012	0.03	0.023	ns
HbA_{1c} (%)	5.85±0.78	6.63±1.70	6.24±0.76	0.049	0.03	0.03	ns
HOMA-IR	4.69 ± 2.64	9.5 ± 7.85	8.49 ± 4.05	0.004*	0.005	0.003	ns
TBARS (μM)	1.06 ± 0.09	1.69 ± 0.83	1.53 ± 0.20	0.01*	0.01	0.001	ns
SOD (U/mg protein)	81.92 ± 39.98	50.87 ± 23.08	72.26 ± 32.71	0.02*	0.05	ns	ns

The data are the mean ± S.D. (or the percentage of 95 enrolled patients). Fasting plasma samples were collected from all 95 patients participating in the study. The groups are as follows: ST, steatosis; SH, steatohepatitis; SH+F, steatohepatitis plus fibrosis, according to the criteria of Matteoni and co-workers. NAFLD fibrosis severity score = 1.75+ [0.037 × age (years)] + [0.094 × BMI (kg m^{-2})] + [1.13 × diabetes (yes = 1, no =0)] + [0.99 × (AST/ALT) ratio] − [0.013 × platelets (10^9/l)] − [0.66 × albumin (g dl^{-1})]. The obesity degree (OD) index is the percentage of deviation of the measured body fat mass ($BF\%_{measured}$) from that expected ($BF\%_{expected}$) using the prediction formulae of Deurenberg and colleagues, assuming a BMI of 24.9 kg m^{-2} as the optimal value for non-obese/non-overweight people so that OD = 100% × [($BF\%_{measured}$) − ($BF\%_{expected}$)]/($BF\%_{expected}$). For details and references, please see the online Supporting Information. SAH, systemic arterial hypertension; AST, plasma aspartate aminotransferase; ALT, plasma alanine aminotransferase; HDL-c, plasma high-density lipoprotein cholesterol fraction; LDL-c, plasma low-density lipoprotein cholesterol fraction; TAG, plasma triacylglycerols (in terms of triolein equivalents); HbA_{1c}, percentage of blood glycated hemoglobin; HOMA, homeostatic model assessment; TBARS, plasma thiobarbituric acid reactive substances; SOD, plasma superoxide dismutase activity. *Differences between groups were assessed by ANOVA; LSD was used for the *post hoc* test, and Bonferroni's correction was applied. Nonparametric comparisons were evaluated by Kruskal-Wallis ANOVA. ns = not significantly different.

although the complete sequence of events linking obesity to inflammation and insulin resistance has not been fully elucidated, the mechanism by which excess lipids/fuels trigger low-grade inflammation in both adipocyte and liver, which contributes to impaired insulin responsiveness, involves the activation of c-Jun NH2-terminal kinases (JNKs), endoplasmic reticulum (ER) stress, the unfolded protein response (UPR), ceramide, and the low-grade inflammatory response in both humans and rodents (9). In fact, the impaired response of cells from diabetic patients to stress (e.g., high blood glucose and fatty acid levels) is associated with the activation JNK cascades, whereas TNFα-elicited JNK activation is a major constituent of free fatty acid-induced insulin resistance (10).

If obesity operates through JNK activation, which feeds forward to systemic inflammation, then stress (inflammation)-induced expression of the 70-kDa family of heat shock proteins (HSP70) works in the opposite direction. In addition to the now classical molecular chaperone action, the most remarkable intracellular effect of HSP70 is its anti-inflammatory action under stressful situations. Accordingly, HSP70 blocks nuclear factor κB (NF-κB) activation at different levels, for example, by impeding inhibitor of κB (IκB) phosphorylation [see, for instance, Ref. 11] and by directly binding to IκB kinase gamma (IKKγ) (12). These effects lead to the inhibition of downstream inflammatory signals. These observations are corroborated by the finding that HSP70 assembles with the liver NF-κB/IκB complex in the cytosol, thus hindering further transcription of NF-κB-dependent genes. This situation is the case for TNFα and inducible nitric oxide synthase (NOS2) genes that increase severe inflammation in rats (12). Additionally, stress-induced HSP70 inhibits JNK-dependent signal transduction, leading to programmed cell

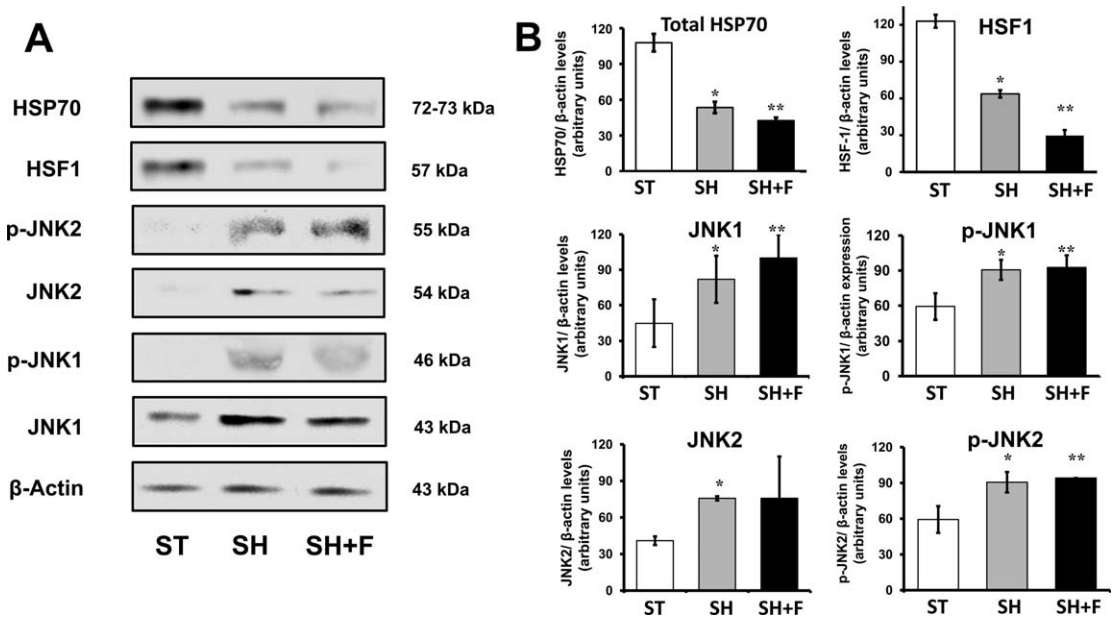

Figure 1 Visceral adipose tissue immunocontents of total HSP70, HSF1, and JNK1/2. For the immunoblot analysis of protein expressions, tissue biopsies were performed on samples from 22 of 95 enrolled patients. Six of these patients had steatosis (ST), ten had steatohepatitis (SH), and six had steatohepatitis plus fibrosis (SH+F). Antibodies to HSP70 detected both the constitutive cognate HSP73 (HSC70) and the inducible HSP72 (HSP70) forms. Antibodies to HSF1 recognized the total (phosphorylated and unphosphorylated) HSF1 forms, whereas the anti-JNK antibodies were specific for either JNK (1 and 2) or diphosphorylated activated JNKs (p-JNK1 and p-JNK2). A representative gel from 1 sample of 22 patients is shown in panel A. The quantification results of the immunodetected proteins in relation to β-actin contents are presented as the means ± S.D. of 22 samples in panel B. $^{*}P < 0.05$ for the comparison between the ST and SH groups; $^{**}P < 0.05$ for the comparison between the ST and SH+F groups by ANOVA.

death in humans (13). The marked anti-inflammatory action of intracellular HSP70 also explains why cyclopentenone prostaglandins (cp-PGs), which are physiological inducers of HSP70 expression, are powerful anti-inflammatory autacoids (14,15). Nonetheless, one of the most striking observations of obesity states is decreased HSP70 expression in both the skeletal muscle (16) and adipose tissue of obese patients (17), which is consistently associated with insulin resistance. Thus, enhanced HSP70 expression has been convincingly demonstrated to protect against obesity-induced insulin resistance in both humans and animal obesity models, whereas pharmacological (*e.g.,* the hydroxylamine derivative BGP-15, which is now under clinical trial) and physiological (hyperthermic, hot tub) treatments are being tested as possible therapeutic approaches for humans with type 2 diabetes (18).

The interconnection between obesity, inflammation and HSP70 pathways encompasses a much more complex network that operates at the gene regulatory level. The promoter region of the TNFα gene contains a heat shock transcription factor-1 (HSF1) binding site that represses TNFα transcription; thus, the loss of this repressor results in sustained TNFα expression (19). Hence, HSF1 knockout is associated with a chronic increase in TNFα levels and with increased susceptibility to endotoxin challenge, at least in murine models. The opposite regulation of this network has also been reported; TNFα may transiently repress HSF1 activation (20). Furthermore, JNK1 was irrefragably demonstrated to phosphorylate HSF1 in its regulatory domain, causing the suppression of HSF1 transcribing activity in human cells (21), whereas HSP70 prevents apoptosis by inhibiting JNK-dependent pathways.

Taken together, the above observations led us to investigate whether HSP70 pathways could be impaired in the liver and adipose tissue of NAFLD patients, thus allowing JNK-triggered inflammatory signals to reach metabolic tissues. Moreover, systemic oxidative stress markers were analyzed to assess the relation between HSP70-elicited anti-inflammation and NAFLD progression.

Methods

Ninety-five adult patients (75 women/20 men) with a diagnosis of severe (type 3) obesity who underwent bariatric surgery at the Center for Obesity and Metabolic Syndrome of São Lucas Hospital (COM—PUC/RS, Porto Alegre, RS, Brazil) were included in the study. All 95 patients were submitted to intraoperative liver biopsy to confirm the clinical diagnosis of NAFLD (please see below). According to histological criteria, volunteers were divided into the following groups: steatosis (ST), steatohepatitis (SH) and steatohepatitis with fibrosis (SH+F). Patients with evidence of excessive alcohol use ($\geq$10 g day^{-1}) or with other causes of liver disease (e.g., hepatitis B, hepatitis C, or autoimmune liver disease), as well as those patients receiving treatment with PPAR-γ agonists, were excluded. Clinical, plasma and NAFLD scoring studies were performed in all patients ($N = 95$), whereas 22 of 95 patient samples were randomly assigned among NAFLD groups (at least $N = 7$ per group) for molecular and immunofluorescence analyses. Ethical questions and patient characteristics, as well as manipulation, histopathology, and sample analyses, including immunoblotting, immunohistochemistry, biochemical evaluations, and statistics, are fully described in the online Supporting Information.

TABLE 2 Correlations between the HSP70, HSF1, JNK1, and p-JNK1 immunocontents in tissue biopsies and either the NAFLD progression or NAFLD fibrosis score

Spearman's rank correlation		p-JNK1	JNK1	HSP70	HSF1§	Score	Progression
(A) Adipose tissue							
p-JNK1	Spearman's ρ Coefficient	1.000	0.983**	−0.995	−0.952**	0.713*	**0.893****
	σ (2-tailed)	-	0.0014	0.0014	0.0013	0.0011	0.0012
	N	22	22	22	22	22	22
JNK1	Spearman's ρ Coefficient	0.983**	1.000	−0.997*	−0.992**	0.828	**0.960****
	σ (2-tailed)	0.0014	-	0.0014	0.0013	0.0011	0.0013
	N	22	22	22	22	22	22
HSP70	Spearman's ρ Coefficient	−0.995	−0.997*	1.000	0.978**	−0.781	**−0.934***
	σ (2-tailed)	0.0014	0.0014	-	0.0013	0.0011	0.0013
	N	22	22	22	22	22	22
HSF1	Spearman's ρ Coefficient	−0.952**	−0.992**	0.978 **	1.000	−0.894**	**−0.988****
	σ (2-tailed)	0.0013	0.0014	0.0013	-	0.0012	0.0014
	N	22	22	22	22	22	22
Score	Spearman's ρ Coefficient	0.713*	0.828	−0.781	−0.894**	1.000	**0.953****
	σ (2-tailed)	0.0010	0.0011	0.0011	0.0012	-	0.0013
	N	22	22	22	22	22	22
Progression	Spearman's ρ Coefficient	**0.893****	**0.960****	**−0.934***	**−0.988****	**0.957****	1.000
	σ (2-tailed)	0.0011	0.0014	0.0013	0.0014	0.0013	-
	N	22	22	22	22	22	22
(B) Liver							
p-JNK1	Spearman's ρ Coefficient	1.000	0.885**	−0.354	−0.968**	0.447*	**0.647****
	σ (2-tailed)	-	0.000	0.106	0.001	0.037	0.001
	N	22	22	22	22	22	22
JNK1	Spearman's ρ Coefficient	0.885**	1.000	−0.437*	−0.985*	0.403	**0.583****
	σ (2-tailed)	0.000	-	0.042	0.001	0.063	0.004
	N	22	22	22	22	22	22
HSP70	Spearman's ρ Coefficient	−0.354	−0.437*	1.000	0.975**	−0.313	**−0.456***
	σ (2-tailed)	0.106	0.042	-	0.001	0.156	0.033
	N	22	22	22	22	22	22
HSF1[a]	Spearman's ρ Coefficient	−0.968 **	−0.985	0.975**	1.000	−0.343	**−0.956 ****
	σ (2-tailed)	0.001	0.001	0.001	-	0.843	0.001
	N	22	22	22	22	22	22
Score	Spearman's ρ Coefficient	0.447*	0.403	−0.313	−0.343	1.000	**0.795****
	σ (2-tailed)	0.037	0.063	0.156	0.843	-	0.000
	N	22	22	22	22	22	22
Progression	Spearman's ρ Coefficient	**0.647****	**0.583****	**−0.456***	**−0.956 ****	**0.795****	1.000
	σ (2-tailed)	0.001	0.004	0.033	0.001	0.000	-
	N	22	22	22	22	22	22

Correlations between HSP70, HSF1, JNK1 and p-JNK1 immunocontents in patient biopsies and either NAFLD progression (ST = 1; SH = 2; SH+F = 4) or NAFLD fibrosis severity score were approached. The samples were obtained from 22 of 95 patients enrolled in the study. NAFLD and fibrosis scores were as described in the legend of Table 1. Spearman's rank correlation (followed by Spearman's ρ coefficient) was calculated ($\pm$ σ). Bi-tailed Student's t test was used to estimate the significance of the calculated coefficients. For the comparisons, $^{*}P < 0.05$ and $^{**}P < 0.01$. For details and references, please see the online Supporting Information. A, adipose tissue immunoblots; B, liver immunoblots. §HSF1 contents in liver samples were evaluated only by immunofluorescence.

Results

General

Anthropometric and biochemical data from the enrolled patients are presented in Table 1. Of the 95 type III obese patients (BMI $>$ 45 kg m^{-2}), 79% were women, and 21% were men. According to the histological characterization, the patients were classified as presenting steatosis (ST, 28.4%), steatohepatitis (SH, 40%) or steatohepatitis accompanied by fibrosis (SH+F, 31.6%). Despite marked differences in NAFLD presentation, no detectable differences were observed for the BMI, waist circumference, and the percentage of body fat, obesity degree, or plasma lipid contents. However, similarities were not observed for the data regarding cardiovascular risk factors and glycemic control; the SH and SH+F patient groups displayed increased insulin resistance (HOMA-IR), glycated hemoglobin, and fasting glycemia and insulinemia

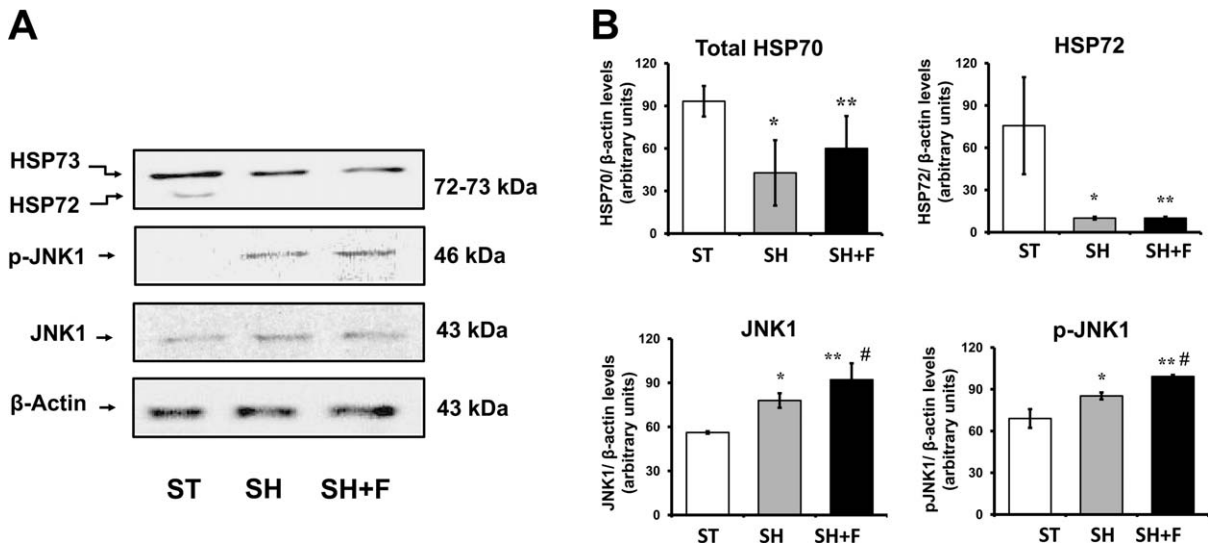

Figure 2 Hepatic tissue immunocontents of HSP72/HSP73 and JNK1/p-JNK1. For the immunoblot analysis of protein expressions, tissue biopsies were performed on samples from 22 of 95 enrolled patients. The samples were as described in the legend of Figure 2. Antibodies to HSP70 detected both the constitutive cognate HSP73 (HSC70) and the inducible HSP72 (HSP70) forms. Anti-JNK antibodies were specific for either JNK (1 and 2) or the diphosphorylated activated JNKs (p-JNK1 and p-JNK2). A representative gel from 1 sample of 22 patients is shown in panel A. The quantification results of the immunodetected proteins in relation to β-actin contents are presented as the means ± S.D. of 22 samples in panel B. $^{*}P < 0.05$ for the comparison between the ST and SH groups; $^{**}P < 0.05$ for the comparison between the ST and SH+F groups; $\#P < 0.05$ for the comparison between the SH and SH+F groups by ANOVA.

compared with those parameters in the ST group (Table 1). The HOMA-IR values in NASH (nonalcoholic steatohepatitis = SH and SH+F) patients were two-fold higher than those values found in ST obese individuals ($P < 0.004$). Moreover, the prevalence of systemic arterial hypertension (SAH) and diabetes was also much higher in NASH patients than in ST patients.

The activity levels of plasma liver enzymes were also higher in NASH patients compared with those levels in the ST group, as expected, denoting a higher degree of hepatic damage and accompanying systemic oxidative stress, as evaluated by TBARS, which is a simple technique that allows the degree of lipoperoxidation to be assessed. This finding was confirmed by a slight but significant decrease in the activity of the antioxidant enzyme superoxide dismutase (SOD), particularly in the SH group, compared with that of ST patients (Table 1).

The incremental severity of inflammatory disease (from ST to SH and SH+F) is clearly denoted by characteristic leukocyte infiltration within the hepatic tissue of these patients (as typified in Supporting Information Figure S1).

HSP70 vs. JNK status in the adipose tissue of NAFLD patients

Consistent with the proposal that a progressively higher degree of liver inflammation among NAFLD patients could be related to a parallel rise in the inflammatory status in adipose tissue due to a loss of function of HSP70 anti-inflammatory and cytoprotective activity, we investigated HSP70 protein contents in biopsies of visceral adipose tissue from these patients (Figure 1). Notably, total HSP70 (HSP72+HSP73) protein contents in adipose tissue of NAFLD patients inversely correlated with disease progression ($\rho = -0.934$, $P < 0.05$) and markedly decreased in the NASH patients compared with the ST groups ($P < 0.05$), which correlated ($\rho = -0.978$) with the conspicuous suppression of HSF1 immunocontents in adipose tissue from the same patients, as depicted in Table 2. Furthermore, when the anti-HSP72 antibody clone C92F3A-5 (which specifically recognizes the 72 kDa form of HSP70) was used, we were not able to detect the presence of HSP70 in adipose tissue (data not shown). Paralleling these observations, JNK1 and JNK2 (both total and Thr183/Tyr185-diphosphorylated/activated forms, *p*-JNKs) were enhanced in adipose tissue from the same patients ($P < 0.05$). Table 2 summarizes all the correlations between the groups.

HSP70 vs. JNK status in the hepatic tissue of NAFLD patients

Liver biopsies from NAFLD patients ($N = 22$) were also analyzed for HSP70 (HSP72 and HSP73 forms) and JNK (JNK1 and JNK2; both total and diphosphorylated activated forms) protein contents. Similar to that observed in adipose tissue from the same patients, total HSP70 (HSP72+HSP73) protein contents were found to be slightly but significantly decreased as NAFLD progresses ($\rho = -0.456$, $P < 0.05$). This finding is associated with a significant reduction in the levels of the inducible form of HSP70 (HSP72), whereas the cognate HSP70 form (HSP73) only slightly decreased (Figure 2). Once again, as observed in adipose tissue, the liver JNK1 and p-JNK1 contents were reciprocally enhanced in relation to HSP70 levels (please see Table 2 for the correlations), thus suggesting that both JNK1 expression and activation were augmented

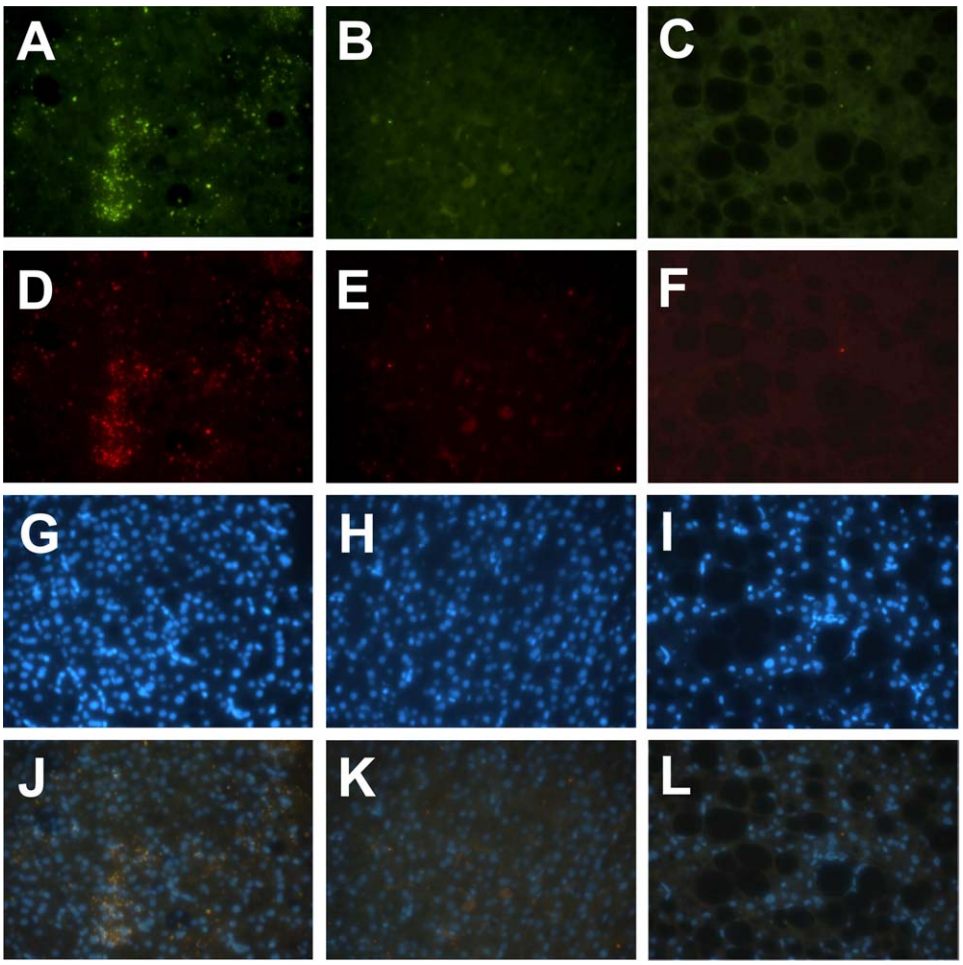

Figure 3 Co-localization of HSP70- and HSF1-positive cells in the livers of NAFLD patients. Liver biopsies were collected and fixed as described in the Methods section and then probed with anti-HSP70 (FITC, green; both cognate HSP73 and inducible HSP72 forms) and anti-HSF1 (red) antibodies. Nuclei were evinced with DAPI counterstaining. The groups are as follows: steatosis (ST): **A**, **D**, **G**, and **J** (merged); steatohepatitis (SH): **B**, **E**, **H**, and **K** (merged); steatohepatitis plus fibrosis (SH+F): **C**, **F**, **I**, and **L** (merged). Representative immunohistochemistry sections from 22 patients are shown. Samples were as described in the legend of Figure 2. Original magnification: ×40.

during NAFLD progression. JNK2 was not detected in the liver tissues of these patients.

We analyzed NAFLD liver biopsies for HSP70 and HSF1 contents using immunohistochemistry (IHC) and immunofluorescence (IF). As shown in Figure 3, a progressive decrease in HSP70 immunoreactivity was observed in the livers of the patients as NAFLD progresses from ST to SH and SH+F (Figure 3A-C); this decrease is similar in magnitude to the rate of decrease in the number of HSF1-positive cells (Figure 3D-F). This possible correlation was also tested, with $\rho = -0.456$ ($P < 0.05$) for HSP70 and with $\rho = -0.956$ ($P < 0.01$) for HSF1 (Table 2). The IF analysis also indicated the co-localization of HSP70 and HSF1 in the slices (Figure 3J-L), thus suggesting a causal effect of decreased HSF1 over HSP72 (the inducible form of HSP70) immunodetection because HSP73 expression is not influenced by HSF1 activation/expression (22). This observation reinforces immunoblot analyses performed with the same samples in which HSP72 was the HSP70 form most affected by NAFLD progression (Figure 2).

The IF analyses of liver biopsies from NAFLD patients (Figure 3) also revealed an inconsistency between the cellular nature of HSP70/HSF1-positive cells and hepatocytes (expected to respond to NAFLD by altering HSP70 expression). In all the examined slices, the co-localization of HSP70 and HSF1 immunostaining (Figure 3J-L) was not on the same cellular structures as were hepatocytes. In fact, hepatocytes were clearly in another histological plane (hepatocytes are the cells whose nuclei are blue-stained by the fluorophore DAPI (Figure 3G-I) and were found to be above the "orange cell" plane of Figure 3J-L). Because of the shape of the structures (small cells) co-localizing HSP70 and HSF1 immunodetection, we conjectured that the cells affected by the progressively decreasing effect of NAFLD over HSP70/HSF1 contents could be Kupffer cells. In fact, as shown in Figure 4, the NAFLD degree-dependent reduction of

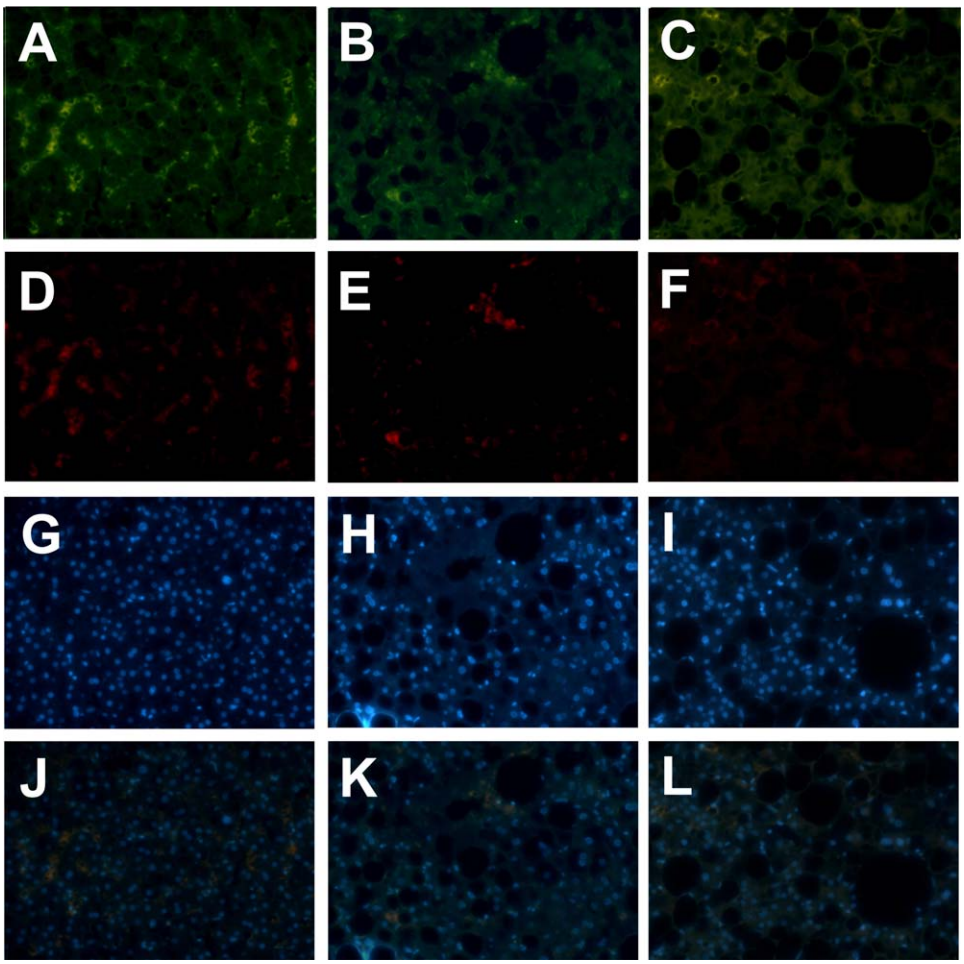

Figure 4 Co-localization of HSP70- and CD14-positive cells in the livers of NAFLD patients. Liver biopsies were collected and fixed as described in the Methods section and then probed with anti-HSP70 (FITC, green; both cognate HSP73 and inducible HSP72 isoforms) and anti-CD14 (red) antibodies. Nuclei were evinced with DAPI counterstaining. Phase contrast images from the same sections are also shown. The groups are as follows: steatosis (ST): **A**, **D**, **G**, and **J** (merged); steatohepatitis (SH): **B**, **E**, **H**, and **K** (merged); steatohepatitis plus fibrosis (SH+F): **C**, **F**, **I**, and **L** (merged). Representative immunohistochemistry sections from 22 patients are shown. Samples were as described in the legend of Figure 2. Original magnification: ×40.

HSP70 in liver slices (Figure 4A-C) did co-localize with small $CD14^+$ cells (Figure 4D-F and Figure 4M-O), which is similar to the decreasing effect observed on the "orange cells" of Figure 3J-L.

When fluorescence intensities measured in liver slices were normalized by the hepatocyte number in the same fields, a sharp decrease in HSP70+ cells that inversely correlated with the progress of hepatic disease was also observed. Additionally, decreased HSP70 contents corresponded with ($\rho = -0.975$, $P < 0.01$; Table 2) a similar reduction in HSF1 contents (Figure 5A). Interestingly, in terms of the number of hepatocytes, the ratio of HSP70- to HSF1-positive cells, was unaltered by NAFLD progression (Figure 5C). The same comparison was performed for the fluorescence intensity in HSP70+/CD14+ cells. As depicted in Figure 5B, HSP70+ cell-derived fluorescence significantly decreased with NAFLD progression from ST to SH. No difference in normalized HSP70 contents was observed between the SH and SH+F groups, thus indicating that HSP70 reduction is dependent on the progression of inflammation, regardless of the presence of fibrosis. It is of note, however, that the number of CD14+ cells (normalized to hepatocytes) remained constant, suggesting that the HSP70 reduction in CD14+ cells was not due to a reduced number of small CD14+ cells (Figure 5D).

Although hepatocytes also express CD14, the cells co-localizing HSP70 and CD14+ (Figures 3 and 4) are clearly not hepatocytes. This co-location in the ST patient biopsies is even clearer when a low-magnification image merged with phase contrast micrograph is analyzed, as in Supporting Information Figure S2. Therefore, we believe that NAFLD progression negatively influences HSP70 contents in Kupffer cells, although hepatocytes seem to continue to express some HSP70 (but in CD14-negative cells in our preparations). Table 3 summarizes all the above results.

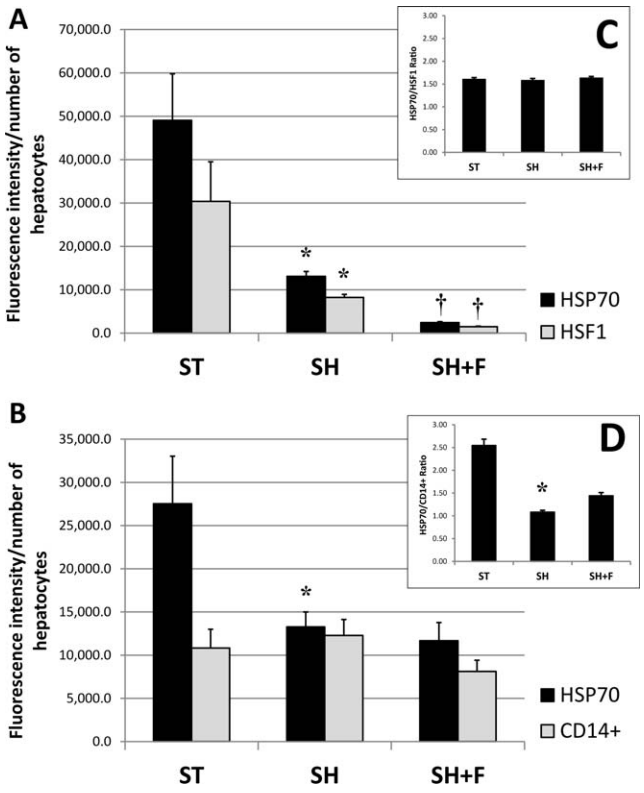

Figure 5 Quantification of fluorescence intensity normalized to number of hepatocytes. Relative fluorescence intensity of liver biopsies probed for (**A**) HSP70 and HSF1 co-localization or for (**B**) HSP70 and CD14 co-localization are shown. The data were collected from the same 22 patients whose representative immunofluorescence panels are depicted, respectively, in Figures 3 and 4. The values, which are presented as the means ± S.D. of 22 samples, are presented as the fluorescence intensity measured in each micrograph divided by the number of hepatocytes detected in the same fields. Inset C shows the HSP70 to HSF1 ratio from values depicted in panel A, whereas inset D displays the HSP70 to CD14 ratio from panel B. *$P < 0.05$ for the comparison between the ST and SH groups; †$P < 0.05$ for the comparison between the SH and SH+F groups by ANOVA.

Discussion

Although the body fat percentage and plasma lipids may have central roles in NAFLD pathogenesis (2), the present results did not provide a reliable marker for following NAFLD progression from ST to NASH (SH and SH+F). Accordingly, the present data demonstrated that NAFLD may be related to a state of cellular stress and inflammation, whether in adipose tissue and liver or somewhere else, that can be traced in the plasma as alterations in lipoperoxidation. In fact, TBARS measurements, which are a simple but good estimate of lipoperoxidation/malondialdehyde produced throughout the body (systemic oxidative stress), were elevated in NASH plasma samples compared with ST plasma samples, which correlated with the degree of insulin resistance (HOMA-IR) and co-morbidities, such as diabetes and arterial hypertension prevalence (Table 1). In contrast, the plasma levels of SOD, which is an important antioxidant produced in response to oxidative stress, did not correlate with NAFLD progression from its simple ST form toward the more inflammatory SH+F form. Curiously, plasma SOD levels positively correlate with the degree of severity of oxidative stress in metabolic syndrome, with clear augmentation in the livers of NAFLD patients (23).

However, the most striking observation from the present study was the first demonstration that the HSF1-HSP70 axis is progressively suppressed in the adipose tissue and livers of obese patients as NAFLD evolves from ST toward SH+F. Moreover, this suppression strongly correlated (Table 2) with the degree of enhancement of total JNK1 and JNK2 immunocontents in adipose tissue (Figure 1), followed by similar increases in the amounts of Thr183/Tyr185-diphosphorylated activated p-JNK1 and p-JNK2 in the same tissue (Figure 1).

A similar pattern of HSP70 reduction, paralleled by proportionate JNK1 activation, was observed in the livers of NAFLD patients. However, in contrast to adipose tissue, the impairment of the inducible form of HSP70 (HSP72) was much more evident in the liver than in adipose tissue. The presence of JNK2 was not verified in the liver (cf., Figures 1 and 2), consistent with the notion that JNK1, but not JNK2, promotes the development and aggravation of NAFLD, at least in mice (24).

Taken together, the above findings may suggest a causal effect of decreased HSF1 expression over HSP72 for NAFLD progression because HSP72 expression is entirely dependent on induction via the HSF1 pathway [in contrast to that observed in the constitutive HSP73 form, whose expression is HSF1-independent (22)]. Because of HSF1/HSP70 reduction, JNK-based pro-inflammatory pathways may be derepressed, thus allowing for enhanced oxidative stress and worsening of the disease, considering that HSF1 may suppress TNFα expression in the murine model (19). In contrast, TNF-α may impede HSF1 activation (20) and transcribing activity in human cells (21). Hence, any factor that disrupts HSF1 biochemical pathways easily triggers a vicious cycle of inflammation, oxidative stress, tissue damage and so on.

Oxidative stress associated with mitochondrial dysfunction and ER stress are triggering factors for the increased expression and activation of JNK and NF-κB, with the concomitant development of a more pro-inflammatory state in humans (6,25). In this regard, we have recently shown that increased oxidative and nitrosative stress and reduced antioxidant enzyme activity in rodent model of diabetes are the leading causes of redox imbalance-elicited NF-κB activation, which evolves to animal liver tissue damage in (26) that perpetuates inflammation. In fact, the selective inactivation of both JNK1 and JNK2 in the adipose tissue of mice protects the animals against a diet-induced increase in adiposity and improves insulin sensitivity in both liver and skeletal muscle (27).

In mammalian tissues, the expression of HSP70s is constitutive (HSP73 = HSC70) and stress-inducible (HSP72). Although both HSP70 forms work as molecular chaperones with anti-inflammatory properties, situations that displace cells from homeostasis (e.g., heat shock, heavy metals, and inflammatory signals) quickly trigger HSF1-dependent transcription of much HSP72 to counteract these cellular insults. Therefore, a reduced capacity for stress-induced HSP72 expression is at the center of inflammation and insulin resistance in both the skeletal muscle (16) and adipose tissue of obese patients (17). In fact, HSP72 expression plays a key role in blocking inflammation and in preventing insulin resistance in the context of genetic obesity or high-fat feeding (18).

However, the above considerations raise a central question: what is the mechanism underlying decreased HSF1-mediated HSP70

TABLE 3 Summary of clinical, plasma, and liver results

	NAFLD progression (Matteoni's ranking)		
Parameter investigated	**ST (type 1)**	**SH (type 2)**	**SH+F (type 4)**
Diabetes prevalence (%)	33.3%	74.4% [↑123% *vs* ST]*	79.3%$^{(ns)*}$
HOMA-IR	4.69 ± 2.64	9.5 ± 7.85 [↑103% *vs* ST]*	8.49 ± 4.05$^{(ns)*}$
HbA_{1c} (%)	5.85±0.78	6.63±1.70 [↑13% *vs* ST]*	6.24 ± 0.76$^{(ns)*}$
SAH prevalence (%)	7.4%	60.5% [↑716% *vs* ST]*	56.0%$^{(ns)*}$
Total HSP70 levels in the liver (IB)	93.27 ± 11.5	42.75 ± 23.22 [↓54% *vs* ST]*	59.99 ± 21.68$^{(ns)*}$
HSP72 levels in the liver (IB)	76.64 ± 34.83	10.00 ± 3.10 [↓87% *vs* ST]*	10.00 ± 3.87$^{(ns)*}$
HSP70+ cells in the liver (IF)	49,070 ± 10,722	13,092 ± 1,133 [↓73% *vs* ST]*	2,440 ± 211†*
HSF1+ cells in the liver (IF)	30,386 ± 9,128	8,233 ± 712 [↓[↓73% *vs* ST]*	1,486 ± 129†*
CD14+ cells in the liver (IF)	10,883 ± 2,167	12,283 ± 1,842 [not altered *vs* ST]	8,112 ± 1,298$^{(ns)}$
HSP70+/CD4+ cells in the liver (IF)	27,534 ± 5,502	13,274 ± 1,725 [↓52% *vs* ST]*	11,672 ± 2,101$^{(ns)*}$
JNK1 levels in the liver (IB)	56.18 ± 2.29	77.96 ± 4.57 [↑39% *vs* ST]*	92.07 ± 10.29†*
Activated *p*-JNK1 in the liver (IB)	69.00 ± 6.86	85.23 ± 2.86 [↑24% *vs* ST]*	99.20 ± 1.14†*

IB: immunoblot values are presented as the means ± S.D. of the data depicted in Figure 2. IF: immunofluorescence intensity normalized to the number of hepatocytes; the data are presented as the means ± S.D. from the data depicted in Figure 5. [↑] and [↓] represent increased and decreased values, respectively, ($P < 0.05$) with respect to the ST results. *$P < 0.05$ for the comparisons with the ST group and †$P < 0.05$ for the comparisons with the SH group by ANOVA. $^{(ns)}$ = not significantly different when the SH+F group is compared with the SH group.

expression in adipose tissue and liver? Obesity-induced cellular senescence of adipocytes may partly answer this question. We presented this testable hypothesis based on the following observations. A senescent-like state can evolve in fat cells from obese individuals as an adaptation to the metabolic overutilization of fat cells, which resembles cellular aging (28). Moreover, high-fat diet-induced obesity has been shown to induce vascular senescence in mice (29). Fibroblasts from adult segmental progerioid Werner syndrome, which undergo premature senescence, present a strong positive feedback system in which p38-NF-κB pathway overactivation blocks the expression of the RNA-binding factor HuR, which is a potentiating factor for the NAD^+-dependent protein deacetylase sirtuin-1 (SIRT1), in human cells (30,31). In turn, SIRT1 enhances HSF1 expression (31), whereas SIRT1 activation prolongs HSF1 binding to the heat shock promoter by maintaining HSF1 in a deacetylated, DNA-binding competent state (32). In contrast, heat shock itself increases the cellular NAD^+/NADH ratio, leading to the recruitment of SIRT1 to the HSP70 promoter (33). Hence, cellular senescence might occlude HSF1 expression and transcribing activity, consequently repressing a protective anti-inflammatory heat shock response.

The recent findings that hepatocyte senescence predicts NAFLD progression in humans (34) and that hepatocyte senescence is a general marker of human liver cirrhosis (35), which is the next step of NAFLD progression, support the above observations.

Although one cannot discard the possibility that the reduced heat shock response in hepatocytes may account for NAFLD aggravation (36), our results demonstrated that a possible target of decreased HSP70 in the liver could be Kupffer cells (Figures 4 and 5), which may increase hepatic tissue inflammation. In fact, we demonstrated that the HSP70 contents significantly and progressively diminished in small CD14+ cells of NAFLD patients as the disease evolved from ST toward SH+F. Although not completely understood, a hepatic-free radical generation may exacerbate inflammation through Kupffer cell activation. Moreover, an amplified pro-inflammatory response of M1 Kupffer cells may account for the severity of NAFLD and for its progression to NASH, fibrosis, cirrhosis and, eventually, hepatocellular carcinoma (37). Additionally, a growing body of evidence suggests that Kupffer cells critically contribute to NAFLD progression, particularly because abundant or abnormal lipids may confound the recognition of "fatty hepatocytes as dangerous" promoting adverse interactions with these hepatic macrophages (36,38). The senescence hypothesis is also supported by the observation that experimental Kupffer cell ablation produces a scenario that resembles senescence, with a reduction of the hepatic anti-inflammatory response and a predisposition to steatosis and insulin resistance (39).

To our knowledge, this study is the first to demonstrate a clearly negative correlation between the progression of NAFLD to fibrosis and the expression/activation of the HSF1/HSP72 biochemical pathway in both liver and adipose tissues of NAFLD patients. These alterations were associated with reduced antioxidant enzyme activities and with enhanced JNK1 and JNK2 expression in the adipose tissue and JNK1 expression in the liver. HSP70 suppression also positively correlated with poor maintenance of glucose homeostasis (Table 1), which is notable because weight gain and the baseline HOMA are independent predictors for the development of NAFLD (40).

Finally, these observations may have an important diagnostic value for NAFLD patients because the "HSP70 status" in the circulating blood of human patients is relatively easy to assess (please cf., Ref. 17 and 36). Clinical and translational confirmatory procedures are currently under evaluation in our laboratories.

Clinical Perspectives

- During the establishment of obesity and visceral adiposity, a conspicuous and increasing activation of inflammatory pathways occurs in metabolic organs, such as adipose tissue, skeletal muscle and liver, thus leading to a state of systemic low-grade

inflammation that accompanies the impairment of insulin responsiveness and NAFLD.

- In the present work, the heat shock protein biochemical pathway, whose activity is powerfully cytoprotective and anti-inflammatory, was found to be depressed and negatively correlated with NAFLD progression in both the liver and adipose tissue of NAFLD patients.
- These observations may have an important diagnostic value for severely obese and NAFLD patients because the "HSP70 status" may be assessed in the circulating blood of human patients using a small blood drop.O

References

1. Pi-Sunyer FX. The obesity epidemic: pathophysiology and consequences of obesity. *Obes Res* 2002;10 (Suppl 2):97S-104S.
2. Vernon G, Baranova A, Younossi ZM. Systematic review: the epidemiology and natural history of non-alcoholic fatty liver disease and non-alcoholic steatohepatitis in adults. *Aliment Pharmacol Ther* 2011;34:274-285.
3. Gregor MF, Hotamisligil GS. Inflammatory mechanisms in obesity. *Annu Rev Immunol* 2011;29:415-445.
4. Xu A, Wang Y, Keshaw H, Xu LY, Lam KS, Cooper GJ. The fat-derived hormone adiponectin alleviates alcoholic and nonalcoholic fatty liver diseases in mice. *J Clin Invest* 2003;112:91-100.
5. Tarantino G. Should nonalcoholic fatty liver disease be regarded as a hepatic illness only? *World J Gastroenterol* 2007;13:4669-4672.
6. Boden G, Duan X, Homko C, et al. Increase in endoplasmic reticulum stress-related proteins and genes in adipose tissue of obese, insulin-resistant individuals. *Diabetes* 2008;57:2438-2444.
7. Sampey BP, Vanhoose AM, Winfield HM, et al. Cafeteria diet is a robust model of human metabolic syndrome with liver and adipose inflammation: comparison to high-fat diet. *Obesity* 2011;19:1109-1117.
8. Popa C, Netea MG, van Riel PL, van der Meer JW, Stalenhoef AF. The role of TNF-alpha in chronic inflammatory conditions, intermediary metabolism, and cardiovascular risk. *J Lipid Res* 2007;48:751-762.
9. Hotamisligil GS. Role of endoplasmic reticulum stress and c-Jun NH2-terminal kinase pathways in inflammation and origin of obesity and diabetes. *Diabetes* 2005; 54 (Suppl 2):S73-S78.
10. Johnson GL, Nakamura K. The c-jun kinase/stress-activated pathway: regulation, function and role in human disease. *Biochim Biophys Acta* 2007;1773:1341-1348.
11. Chan JY, Ou CC, Wang LL, Chan SH. Heat shock protein 70 confers cardiovascular protection during endotoxemia via inhibition of nuclear factor-kappaB activation and inducible nitric oxide synthase expression in the rostral ventrolateral medulla. *Circulation* 2004;110:3560-3566.
12. Chen HW, Kuo HT, Wang SJ, Lu TS, Yang RC. In vivo heat shock protein assembles with septic liver NF-kappaB/I-kappaB complex regulating NF-kappaB activity. *Shock* 2005;24:232-238.
13. Gabai VL, Meriin AB, Mosser DD, et al. Hsp70 prevents activation of stress kinases. A novel pathway of cellular thermotolerance. *J Biol Chem* 1997;272:18033-18037.
14. Gutierrez LL, Maslinkiewicz A, Curi R, Homem de Bittencourt PI Jr. Atherosclerosis: a redox-sensitive lipid imbalance suppressible by cyclopentenone prostaglandins. *Biochem Pharmacol* 2008;75:2245-2262.
15. Rossi A, Kapahi P, Natoli G, et al. Anti-inflammatory cyclopentenone prostaglandins are direct inhibitors of IkappaB kinase. *Nature* 2000;403:103-108.
16. Bruce CR, Carey AL, Hawley JA, Febbraio MA. Intramuscular heat shock protein 72 and heme oxygenase-1 mRNA are reduced in patients with type 2 diabetes: evidence that insulin resistance is associated with a disturbed antioxidant defense mechanism. *Diabetes* 2003;52:2338-2345.
17. Rodrigues-Krause J, Krause M, O'Hagan C, et al. Divergence of intracellular and extracellular HSP72 in type 2 diabetes: does fat matter? *Cell Stress Chaperones* 2012;17:293-302.
18. Chung J, Nguyen AK, Henstridge DC, et al. HSP72 protects against obesity-induced insulin resistance. *Proc Natl Acad Sci USA* 2008;105:1739-1744.
19. Singh IS, He JR, Calderwood S, Hasday JD. A high affinity HSF-1 binding site in the 5'-untranslated region of the murine tumor necrosis factor-alpha gene is a transcriptional repressor. *J Biol Chem* 2002;277:4981-4988.
20. Knowlton AA. NFkappaB, heat shock proteins, HSF-1, and inflammation. *Cardiovasc Res* 2006;69:7-8.
21. Dai R, Frejtag W, He B, Zhang Y, Mivechi NF. c-Jun NH2-terminal kinase targeting and phosphorylation of heat shock factor-1 suppress its transcriptional activity. *J Biol Chem* 2000;275:18210-18218.
22. Whitesell L, Lindquist S. Inhibiting the transcription factor HSF1 as an anticancer strategy. *Expert Opin Ther Targets* 2009;13:469-478.
23. Perlemuter G, Davit-Spraul A, Cosson C, et al. Increase in liver antioxidant enzyme activities in non-alcoholic fatty liver disease. *Liver Int* 2005;25:946-953.
24. Schattenberg JM, Singh R, Wang Y, et al. JNK1 but not JNK2 promotes the development of steatohepatitis in mice. *Hepatology* 2006;43:163-172.
25. Tarantino G, Caputi A. JNKs, insulin resistance and inflammation: a possible link between NAFLD and coronary artery disease. *World J Gastroenterol* 2011;17:3785-3794.
26. Di Naso FC, Rodrigues G, Dias AS, Porawski M, Fillmann H, Marroni NP. Hepatic nitrosative stress in experimental diabetes. *J Diabetes Complications* 2012;26:378-381.
27. Zhang X, Xu A, Chung SK, et al. Selective inactivation of c-Jun NH2-terminal kinase in adipose tissue protects against diet-induced obesity and improves insulin sensitivity in both liver and skeletal muscle in mice. *Diabetes* 2011;60:486-495.
28. Tchkonia T, Morbeck DE, Von Zglinicki T, et al. Fat tissue, aging, and cellular senescence. *Aging Cell* 2010;9:667-684.
29. Wang CY, Kim HH, Hiroi Y, et al. Obesity increases vascular senescence and susceptibility to ischemic injury through chronic activation of Akt and mTOR. *Sci Signal* 2009;2:ra11.
30. Abdelmohsen K, Pullmann R Jr, Lal A, et al. Phosphorylation of HuR by Chk2 regulates SIRT1 expression. *Mol Cell* 2007;25:543-557.
31. Kim G, Meriin AB, Gabai VL, et al. The heat shock transcription factor Hsf1 is downregulated in DNA damage-associated senescence, contributing to the maintenance of senescence phenotype. *Aging Cell* 2012;11:617-627.
32. Westerheide SD, Anckar J, Stevens SM Jr, Sistonen L, Morimoto RI. Stress-inducible regulation of heat shock factor 1 by the deacetylase SIRT1. *Science* 2009; 323:1063-1066.
33. Raynes R, Pombier KM, Nguyen K, Brunquell J, Mendez JE, Westerheide SD. The SIRT1 modulators AROS and DBC1 regulate HSF1 activity and the heat shock response. *PLoS One* 2013;8:e54364.
34. Aravinthan A, Scarpini C, Tachtatzis P, et al. Hepatocyte senescence predicts progression in non-alcohol-related fatty liver disease. *J Hepatol* 2013;58:549-556.
35. Wiemann SU, Satyanarayana A, Tsahuridu M, et al. Hepatocyte telomere shortening and senescence are general markers of human liver cirrhosis. *FASEB J* 2002;16:935-942.
36. Newsholme P, Homem de Bittencourt PI Jr. The fat cell senescence hypothesis: a mechanism responsible for abrogating the resolution of inflammation in chronic disease. *Curr Opin Clin Nutr Metab Care* 2014;17:295-305.
37. Maina V, Sutti S, Locatelli I, et al. Bias in macrophage activation pattern influences non-alcoholic steatohepatitis (NASH) in mice. *Clin Sci* 2012;122:545-553.
38. Baffy G. Kupffer cells in non-alcoholic fatty liver disease: the emerging view. *J Hepatol* 2009;51:212-223.
39. Clementi AH, Gaudy AM, van Rooijen N, Pierce RH, Mooney RA. Loss of Kupffer cells in diet-induced obesity is associated with increased hepatic steatosis, STAT3 signaling, and further decreases in insulin signaling. *Biochim Biophys Acta* 2009;1792:1062-1072.
40. Zelber-Sagi S, Lotan R, Shlomai A, et al. Predictors for incidence and remission of NAFLD in the general population during a seven-year prospective follow-up. *J Hepatol* 2012;56:1145-1151.